ACS APPLIED MATERIALS & INTERFACES

Research Article

www.acsami.org

Hydrogel Micropattern-Incorporated Fibrous Scaffolds Capable of Sequential Growth Factor Delivery for Enhanced Osteogenesis of hMSCs

Hyun Jong Lee and Won-Gun Koh*

Department of Chemical and Biomolecular Engineering, Yonsei University 50 Yonsei-ro, Seodaemun-gu, Seoul 120-749, South Korea

ABSTRACT: In this study, we developed multi-functional biomimetic tissue engineered scaffolds that are capable of controlling the spatial locations of stem cells and releasing multiple growth factors with a controlled dose and rate of delivery. This novel scaffold was fabricated by combining electrospinning and photolithography and consisted of polycaprolactone (PCL)/gelatin fibers and poly(ethylene glycol) (PEG) hydrogel micropatterns. The utility of this system was investigated in the context of the osteogenesis of human mesenchymal stem cells (hMSCs). When hMSCs were seeded onto hydrogel-incorporated fibrous scaffolds, they selectively adhered and grew only in the fiber region due to the non-adhesiveness of the PEG hydrogel, enabling spatial positioning of hMSCs on a micrometer scale. For osteogenic differentiation of hMSCs, basic fibroblast growth factor (bFGF) and bone morphogenetic protein-2 (BMP-2) were loaded on the fibers and within the hydrogel matrix, respectively, to enable sequential delivery of low doses of bFGF during the early stages and sustained release of BMP-2 for long periods. According to in vitro studies, hMSCs cultured on the scaffolds capable of sequential delivery of bFGF and BMP-2 showed stronger osteogenic commitment in culture than those on scaffolds without any growth factors or scaffolds with single administration of either bFGF or BMP-2 under the same conditions. The results demonstrate that hydrogel-incorporated fibrous scaffolds can provide not only biomimetic structures with micropatterned nanostructures but also a suitable biochemical environment with controlled release of multiple growth factors, which may eventually facilitate the control of stem cell fates for various regenerative therapies.

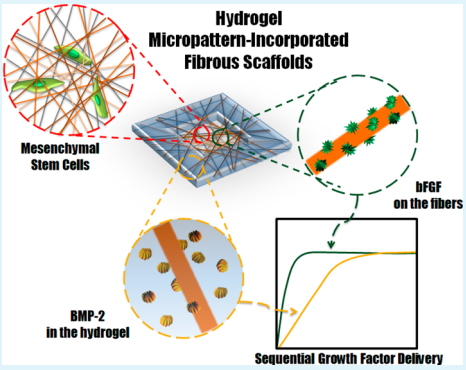

KEYWORDS: *tissue engineering scaffolds, stem cells, hydrogel micropatterns, electrospun fibers, sequential delivery of growth factors, osteogenesis of hMSCs*

INTRODUCTION

Stem cells in vivo reside within an instructive and tissue-specific three-dimensional (3D) microenvironment, termed a "niche", that is composed of insoluble macromolecules of the extracellular matrix (ECM), soluble bioactive factors, and neighboring cells.[1] Because each stem cell's fate is regulated by its natural niche, many researchers have attempted to design niche-mimicking scaffolds in the area of stem cell-based tissue engineering and regenerative medicine. Engineering of artificial niches can be achieved by incorporating architectural and biochemical cues into biomaterials to regulate stem cell behaviors such as proliferation, migration, and differentiation.[2,3]

Architectural cues, such as surface energy, configuration, and composition of biomaterials, are often used to modulate short-term cell functions, such as adhesion, morphology, and proliferation, as well as the spatial locations of stem cells. Within the past decade, a dramatic increase in the resolution of control over scaffold architecture has been achieved through nano/microfabrication technologies.[4,5] Nanoscale topographies such as grooves, ridges, pores, fibers, and pillars can be obtained by using various nanofabrication techniques,[6−12] and it has been shown that the nanotopography promotes and facilitates self-renewal, proliferation, and lineage-specific differentiation of stem cells.[13−15] Among the various nanotopographical substrates, electrospun fibers have gained considerable interest in tissue engineering due to their similarity to the fibrous nature of the ECM.[16] A variety of synthetic and natural biomaterials have been processed into fibrous scaffolds for the growth and differentiation of various stem cells.[17,18] On the other hand, microfabrication techniques combined with surface chemistry have been widely utilized for the spatial control of cells in cell patterning.[19−21] Patterned arrays of single or multiple cell types in culture serve as model systems for exploration of fundamental aspects of cell biology, especially cell−cell, cell−surface, and cell−matrix interactions. Tissue engineering may also require that cells be placed in specific locations to create organized structures.[22] Although numerous studies have prepared electrospun fibers or cellular micropatterns (the former to create biomimetic scaffolds and the latter to control the spatial positions of cells), only a few studies have reported the creation of cellular patterns on electrospun fibrous scaffolds by combining two techniques.[23−25]

Received: March 21, 2014
Accepted: May 27, 2014
Published: June 10, 2014

In addition to scaffold architecture, stem cell fate can be regulated through biochemical cues, such as controlled delivery of various growth factors from the scaffold materials.[26−28] Biochemical cues have been demonstrated to be especially effective for directing stem cell differentiation toward a specialized cell lineage. For example, bone morphogenic proteins (BMPs) play a key role in stimulating bone growth and the differentiation of stem cells into osteoblasts.[29,30] Because tissue formation and repair from stem cells is a complex cascade of events in which a number of growth factors are involved, controlled delivery of combinations of growth factors rather than a single growth factor from scaffolds appears to be a logical strategy to mimic cell niches for applications such as tissue engineering.[31] The sequential or simultaneous delivery of multiple growth factors has been achieved in multiple systems including poly(lactide-*co*-glycolide) (PLG), oligo(poly(ethylene glycol) fumarate), and alginate scaffolds.[32−34] The significance of enhanced osteogenic effect with co-administration of multiple growth factors has been reported by several studies. Enhanced bone formation has been observed with simultaneous application of transforming growth factor-b1 (TGF-β1) and insulin-like growth factor-1 (IGF-1).[35] Similarly, TGF-β3- and BMP-2-loaded alginate scaffolds have significantly enhanced bone formation in comparison with single growth factor-loaded scaffolds.[36] Hasirci et al. reported that sequential delivery of BMP-2 and BMP-7 played a significant role in enhancing osteogenic differentiation of MSCs.[37] Combination of BMP-2 and basic fibroblast growth factor (bFGF) has been widely studied for osteogenesis of hMSCs.[38−43] To optimize the synergetic effects of these two growth factors, some parameters, such as concentration and release timing of each growth factor, should be adjusted. Under non-optimized conditions, the co-delivery of BMP-2 and bFGF can decrease the bone formation of MSCs.[44] Based on previous studies, the optimal condition for osteogenesis is a low dose of bFGF during the early stage of osteogenesis and a sustained release of BMP-2 for long periods.[38,41−43] In spite of numerous studies related to optimizing biochemical cues from various scaffolds, selection of the proper growth factor cocktails and the fine control of their delivery from biomimetic 3D scaffolds are still challenges in stem cell-based tissue engineering.

In this study, our goal was to develop scaffold materials with precisely controlled biomimetic scaffold architecture that regulate the spatiotemporal release of multiple growth factors. To this end, we developed polycaprolactone (PCL)/gelatin fibrous scaffolds incorporated with poly(ethylene glycol)(PEG) hydrogel micropatterns by combining electrospinning and photolithography processes. As a potential application of multiple growth factor-loaded/hydrogel incorporated fibrous scaffolds, we investigated osteogenesis of human mesenchymal stem cells (hMSCs) for bone fracture healing and bone formation. In terms of architectural cues, electrospun fibers provide biomimetic 3D nanotopography, while hydrogel micropatterns are utilized to locate stem cells within well-defined regions by taking advantage of the resistance of PEG hydrogel to cell and protein attachment. Furthermore, our scaffold consists of nano- and micro-structures, which can mimic real tissue composed of several levels of structural hierarchy from the nanometer range to the micro- and centimeter ranges. In addition, in terms of biochemical cues, bFGF and BMP-2 were incorporated into PCL/gelatin fibers and hydrogel micropatterns, respectively, where the release behaviors of each growth factor can be controlled independently. bFGF was immobilized onto fibers via its weak electrostatic interaction with gelatin for early release within 4 days, while BMP-2 was entrapped within hydrogel micropatterns to achieve sustained release over 4 weeks. The main advantage of this scaffold is that this system can not only generate cellular patterns in a biomimetic fibrous network via the different chemistry between cell-repelling PEG hydrogel and cell-adhesive PCL/gelatin fibers but can also realize spatiotemporal release of different growth factors by incorporating each growth factor into spatially distinct hydrogel and fiber domains, respectively, where the dose and rate of delivery are controlled independently.

EXPERIMENTAL SECTION

Materials. Poly(ethylene glycol) (PEG) (MW 3400), acryloyl chloride, hexane, tetrahydrofuran (THF), 2-hydroxy-2-methylpropiophenone (HOMPP), polycaprolactone (PCL) (MW 80 000), glutaraldehyde, 2,2,2-trifluoroethanol (TFE), ethanol, gelatin (from bovine skin, Type B), (3-(4,5-dimethylthiazol-2-yl)-2,5-diphenyltetrazolium bromide (MTT), p-nitrophenyl phosphate (pNPP), sodium hydroxide, sodium chloride, alizarin red S (ARS), paraformaldehyde, tris hydrochloride (Tris-HCl) buffer, Tween 20 and RIPA buffer were purchased from Sigma-Aldrich (Milwaukee, WI, U.S.A.). Phosphate buffered saline (PBS, 0.01 M), Dulbecco's Modified Eagle's Medium (DMEM) with 1.0 g/L glucose, fetal bovine serum (FBS), penicillin/streptomycin, trypsin/ethylenediaminetetra-acetate (trypsin/EDTA), Dulbecco's modified phosphate buffered saline (DPBS), live/dead viability/cytotoxicity kit (L-7013), Alexa Fluor 488, 594 protein labeling kit and 4′,6-diamidino-2-phenylindole (DAPI) were purchased from Invitrogen (Carlsbad, CA, U.S.A.). Basic fibroblast growth factor (bFGF), bone morphogenetic protein-2 (BMP-2) and alkaline phosphatase detection kits were purchased from Millipore (Bedford, MA, U.S.A.). Human Mesenchymal stem cells (hMSCs) were obtained from the American Type Culture Collection (ATCC, Rockville, MD, U.S.A.).

Preparation of the Electrospun PCL/Gelatin Scaffold. Electrospinning was performed as described in our previous report. The differences are briefly summarized as follows.[45,46] An electrospinning solution was prepared by dissolving a mixture of PCL and gelatin (1:1 weight ratio) in TFE to form a 10 % w/v solution. To electrospin PCL/gelatin fibers, a 10 kV positive voltage was applied to the solution via a needle, and a constant feeding rate of solution (0.5 mL/h) was provided by a syringe pump for 20 min. The resulting PCL/gelatin fibers were crosslinked using glutaraldehyde vapor,[47] which was carried out by placing fibers in a sealed desiccator containing 10 mL of 0.5 % w/v aqueous glutaraldehyde solution at room temperature for 24 h. The residual glutaraldehyde was removed in vacuum oven at 50 °C for 24 h. The morphology of the electrospun fibers was observed using scanning electron microscopy (SEM) (JEOL T330A, JEOL, Ltd, Peabody, MA, U.S.A.). The fiber diameters were calculated by measuring the width of fibers in SEM images. The 20 different fibers were chosen and measured using image analysis software (KS 300, Carl Zeiss Inc.).

Incorporation of Hydrogel Patterns into Nanofibers. Hydrogel patterns were fabricated using photolithography technique. PEG-diacrylate (DA) was synthesized from PEG (MW 3400) using a previously published protocol.[48] Precursor solution was prepared by dissolving PEG-DA (50 % w/w) and HOMPP (2 % v/v) in DI water. After precursor solution was dropped onto the electrospun scaffold, a photomask containing an array of microwells was placed on the scaffold and exposed to UV light (365 nm, 300 mW/cm^2, EFOS Ultracure 100 ss Plus, UV sport lamp, Mississauga, Ontario, Canada) for 3 seconds. Finally, hydrogel-incorporated patterned nanofibrous scaffolds were obtained by removing unreacted precursor solution with water. The thickness of fiber mats were obtained from SEM images, while thickness of hydrogel micropatterns were measured using micrometer (on condition that the fiber mats were held between slide-glasses and the thickness of slide-glasses were subtracted).

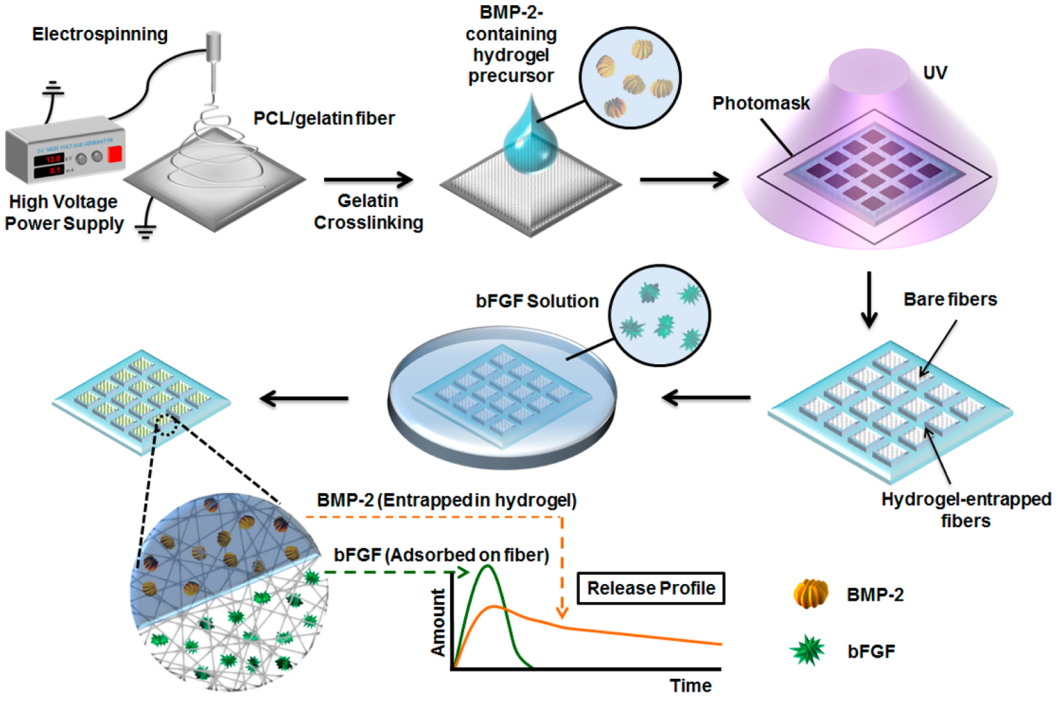

Figure 1. Schematic diagram of preparing dual growth factor-loaded scaffold by using electrospinning and hydrogel micropatterning techniques.

Loading of Growth Factors. BMP-2 was immobilized within the PEG hydrogel patterns via physical entrapment. BMP-2-entrapped hydrogel patterns were prepared by adding 500 ng of BMP-2 to 1 mL of hydrogel precursor solution containing PEG-DA and photoinitiator. This solution underwent the same photopatterning process described in the previous section to produce BMP-2-loaded hydrogel patterns that were incorporated into the nanofibrous scaffolds. bFGF was immobilized onto nanofibrous regions by immersing the patterned scaffolds in 100 ng/mL bFGF solution in cell culture media at 37 °C for 12 h. For the visualization and release study of immobilized growth factors, BMP-2 and bFGF were conjugated with fluorescence molecules using an Alexa Fluor 594 Protein Labeling Kit (Alexa 594-BMP-2) and an Alexa Fluor 488 Protein Labeling Kit (Alexa 488-bFGF), respectively. The amount of loaded growth factors were measured using previously described methods.[46] The overall experimental procedure used to generate these dual growth factor-loaded/hydrogel micropattern-incorporated fibrous scaffolds is described in Figure 1.

Growth Factor Release. The release behaviors of fluorophore-conjugated BMP-2 and bFGF from hydrogel-incorporated nanofiber scaffolds were monitored using fluorescence techniques. Growth factors-loaded scaffolds were incubated in 2.0 mL PBS solution and at predetermined time points (day 1, 4, 7, 14, 21, and 28), 1.0 mL of PBS solution containing released growth factors was collected and the fluorescence intensity of the samples were measured using fluorescence spectroscopy (VictorX5, Perkin Elmer, Waltham, MA, U.S.A.). In addition, fluorescence images of the growth factor-loaded scaffolds were obtained periodically to observe the change of fluorescence intensity in the hydrogel and nanofiber regions by release of BMP-2 and bFGF, respectively. A Zeiss Axiovert 200 microscope equipped with an integrated color CCD camera (Carl Zeiss Inc., Thornwood, NY, U.S.A.) was used to obtain fluorescence images. Image analyses were performed using commercially available image analysis software (KS 300, Carl Zeiss Inc.). When fluorescence intensity was measured from gelatin-containing scaffolds, the fluorescence intensity of gelatin was subtracted from the original fluorescence data because gelatin is auto-fluorescent property.

Cell Culture and Seeding. hMSCs were cultured in DMEM, 10 % v/v FBS, and 1 % v/v antibiotic/antimycotic solution and were incubated at 37 °C in 5 % CO_2 and 95 % air. Growth factor-loaded scaffolds were placed in 24-well plates and sterilized with UV for 30 min. The cells (1.0×10^5 cells/mL) were then seeded onto each scaffold (size of each scaffold was 1×1 cm^2) in the 24-well plates followed by addition of 1 mL of culture medium after 30 min. The hMSC-seeded scaffolds were then moved into new 24-well plates 6 h after cell seeding to exclude the effect of the cells that adhered to the well plate. Cell culture media were replaced every 3 day, and hMSCs were cultured for 21 days. Cells that were seeded on the micropatterned fibrous scaffolds were imaged using a Live/Dead Viability/Cytotoxicity fluorescence assay or DAPI, as described previously.[49]

In Vitro Cell Proliferation. MTT assays were performed to investigate the in vitro proliferation of hMSCs on the hydrogel-incorporated fibrous scaffolds. Briefly, 10 % v/v MTT solution (5 mg/mL) in the culture medium was added to the cell-seeded scaffolds. The samples were incubated for 3 h at 37 °C, and formazan crystals transformed from MTT by mitochondrial reductase were dissolved by DMSO. The absorbance was measured at 570 nm using a microplate reader (Molecular Devices, Sunnyvale, CA, U.S.A.).

ALP Activities and ALP Staining. ALP activity was measured using the p-nitrophenol assay, which is based on the fact that the colorless pNPP is hydrolyzed by alkaline phosphatase (ALP), producing yellow p-nitrophenol. hMSC-containing scaffolds were rinsed with DPBS, and 500 μL RIPA buffer was added to each well. Then, 100 μL of cell lysates was mixed with 100 μL of pNPP and incubated for 30 min at 37 °C in the dark. The reaction was stopped by adding 10 μL of 2 M sodium hydroxide solution and the absorbance at 405 nm was measured using a microplate reader. To observe ALP activities optically, an ALP detection kit was used according to the manufacturer's instructions. The cells on the scaffolds were washed with PBS and fixed with 4 % paraformaldehyde in PBS for 2 min. Fixed cells were rinsed with rinse buffer (20 mM Tris-HCl, pH 7.4, 0.15 M NaCl, 0.05 % Tween 20) and stained with solution consisting of naphthol AS-BI phosphate solution (4 mg/mL in 2 M 2-amino-2 methylpropanediol, pH 9.5), fast red violet solution (0.8 g/L), and water (with volume ratio of 2:1:1) in a dark room for 15 min. The staining solution was aspirated, and the cells were rinsed with rinse buffer. Finally, the cells on the scaffolds were visualized using optical microscopy.

Matrix Mineralization. ARS staining was used to measure the biomineralization of hMSC. After 21 days of hMSC culture, the cells were fixed with 4 % paraformaldehyde for an hour at room

temperature. Then, 40 mM of ARS solution was added and incubated for 5 min at room temperature with gentle shaking. The solution was aspirated and washed with 50 v/v % ethanol. The stained sample was visualized using optical microscopy. To quantify the mineralization, the scaffolds were desorbed using 10% cetylpyridinium chloride for 1 h. The solution was collected and the absorbance at 570 nm was measured.

Statistical Analysis. Each experiment was performed five times, the means of the five experiments were compared using one-way ANOVA, and p-values less than 0.05 were considered statistically significant, and the data were indicated with (*) for $0.01 < p < 0.05$ and (**) for $p < 0.01$, respectively. Error bars represented standard deviation.

RESULTS AND DISCUSSION

Fabrication of Fibrous Scaffolds Incorporating Hydrogel Micropatterns. Fibrous scaffolds patterned with hydrogel were fabricated by combining an electrospinning technique with PEG hydrogel photolithography. First, fibrous scaffolds were obtained by electrospinning a mixture of polycaprolactone (PCL) and gelatin because it is known that incorporation of gelatin produces less hydrophobic fiber than bare PCL fibers, which improves cell adhesion and proliferation onto fibrous scaffolds.[50,51] Because of the water-soluble nature of gelatin, the resultant PCL/gelatin fibers were crosslinked using glutaraldehyde to prevent dissolution of gelatin in the aqueous cell culture environment. The effectiveness of the glutaraldehyde treatment was investigated by observing the morphology of the fibers before and after wetting with water. Before the wetting, un-cross-linked (Figure 2a) and crosslinked fibers (Figure 2b)

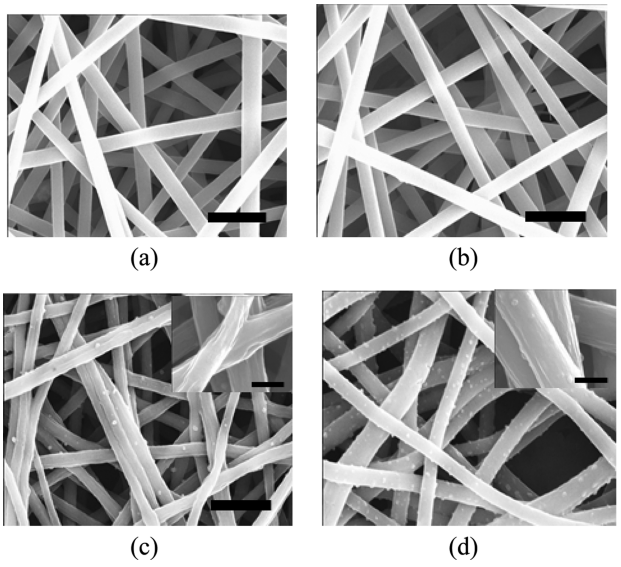

Figure 2. SEM images of (a) un-cross-linked and (b) crosslinked PCL/gelatin fibers right after electrospinning (scale bar: 3 μm). High magnification SEM images of (c) un-cross-linked and (d) crosslinked PCL/gelatin fibers after water wetting (scale bar: 3 μm for low magnification and 1 μm for high magnification).

fibers had smooth surface morphologies, and their diameters were 1.29 ± 0.11 and 1.32 ± 0.11 μm, respectively, with no significant differences observed between the groups. These results indicate that the glutaraldehyde crosslinking does not influence the morphology of the PCL/gelatin fibers. When both types of fibers were immersed in water for 24 h, the diameters of the un-cross-linked fiber significantly decreased to 0.96 ± 0.11 μm and roughened fiber surfaces were observed due to the dissolution of water-soluble gelatin from the fibers as shown in Figure 2c. In the case of the crosslinked PCL/gelatin fibers (Figure 2d), a slight increase of fiber diameter (1.46 ± 0.24 μm) was observed (when compared with original fibers there was no significant difference), which probably resulted from swelling of the crosslinked gelatin. Furthermore, the fibers maintained the original smooth surface morphology without evidence of gelatin dissolution from the fibers.

After successful preparation of crosslinked PCL/gelatin fibrous scaffolds that are not soluble in water, hydrogel micropatterns were incorporated into the fibrous scaffolds using photolithography by utilizing the ability of PEG diacrylate (PEG-DA) to form a gel upon exposure to UV light. Photomasks containing arrays of square patterns (1 mm × 1 mm) separated by 200 μm-wide transparent regions were prepared. The design of the mask allowed only the hydrogel precursor solution below the transparent region of the photomask to be crosslinked and to become a hydrogel micropattern upon exposure to UV light while residual polymer was removed elsewhere in the pattern. Thus, subsequent photopatterning created microwells of fibers separated by hydrogel, as shown in Figure 3a and b.

The wrinkled fiber in SEM image was resulted from the evaporation of water from the PEG hydrogel prior to metal coating for electron microscopy. Because PEG hydrogels have high equilibrium water content (in excess of 80%), they shrank upon drying and made incorporated fibers wrinkled. However, in aqueous environment such as cell culture media, flat morphology of hydrogel-patterned fibrous scaffold was kept maintained. SEM images demonstrated that most of the fibers were inserted at the sides of the hydrogel microstructures, leaving no fibers exposed at the top surfaces of the hydrogel micropatterns. The resultant hydrogel-incorporated fiber scaffolds were obtained as free-standing sheets and could be easily handled. It was found that as the thickness of scaffold became thicker than 200 μm, the masked regions tended to polymerize, resulting in larger hydrogel patterns at the bottom region of fibrous scaffolds. Poor fidelity of hydrogel pattern transfer at the bottom was most likely due to light scattering/diffusion or the mass transfer of free radical species outside of the illuminated area and their subsequent reaction. In the rest of this study, we used scaffolds consisting of 60 μm-thick PCL/gelatin fibers and 100 μm-thick hydrogel micropatterns.

hMSC Culture on the Micropatterned Fibrous Scaffolds. To investigate whether the resulting hydrogel-incorporated PCL/gelatin fibrous scaffolds support adhesion and proliferation of hMSCs, hMSCs were seeded onto scaffolds and cultured for 21 days. An MTT assay was used to evaluate the relative number of viable cells. The MTT assay results indicate that the cells remained viable and were able to proliferate within the micropatterned fibrous scaffolds (Figure 4a). Cultured cells were visualized using a live/dead viability/cytotoxicity fluorescence assay that stains live cells green and dead cells red. Using this assay, the cells within micropatterned scaffolds can be imaged for visualization and assayed for viability simultaneously. As shown in the fluorescence images in Figure 4b, there are many more living cells (green spots) than dead cells (red spots), indicating that most of the adhered cells remained viable on micropatterned fibrous scaffolds (viability was greater than 98 ± 1.5%). Furthermore, all the cells adhered to and proliferated only on PCL/gelatin fiber regions (microwells), generating cellular micropatterns because PEG hydrogel micropatterns effectively prevented cell adhesion,

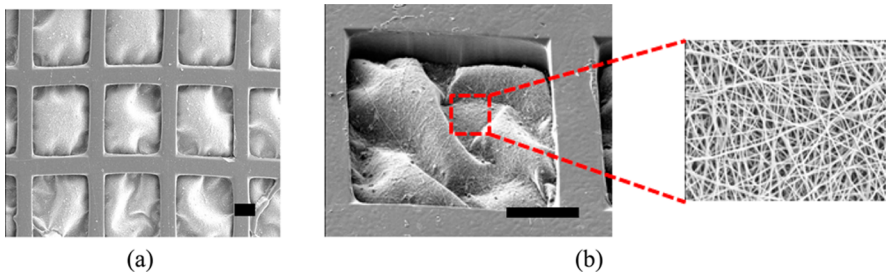

Figure 3. SEM images of hydrogel micropattern-incorporated fibrous scaffold. (a) Low magnification (× 30) image showing multiple microwells consisting of fibrous bottoms and hydrogel walls. (b) High magnification image (× 100) showing single microwell and SEM image of fibers (× 1000). Scale bar is 300 μm.

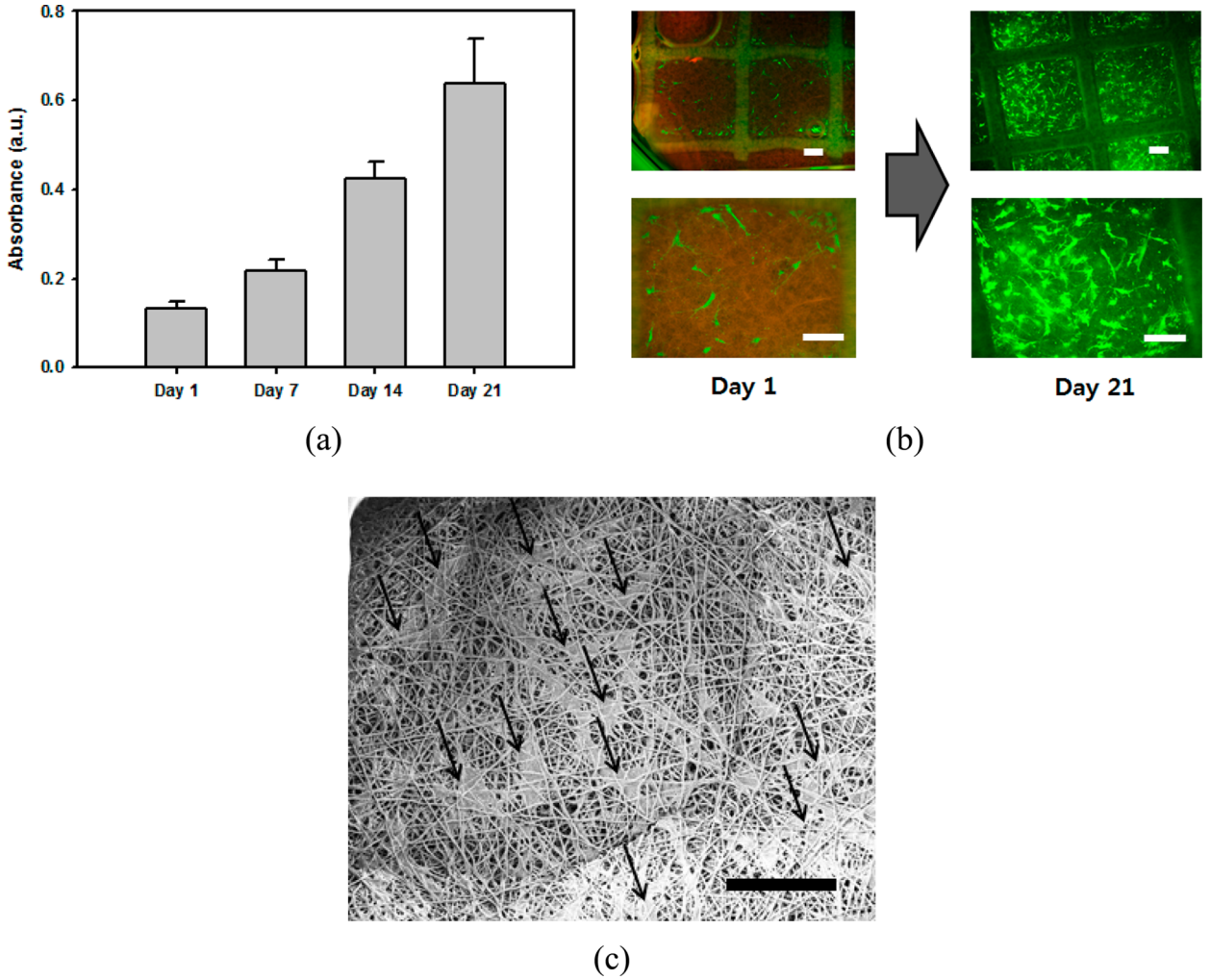

Figure 4. Culture of hMSCs on hydrogel micropattern-incorporated fibrous scaffold. (a) Result of MTT assay at different culture periods. (b) Fluorescence images of hMSCs obtained from live/dead fluorescence viability assay at day 1 and day 21 of culture (scale bar: 200 μm). (c) SEM image showing hMSCs on fibers (arrows indicate the hMSCs, and scale bar = 100 μm).

spreading, and crossover. Micropatterning of PEG hydrogels in the presence of PCL/gelatin fibers underscored the clear contrast between the cell adhesion-resistant PEG hydrogel wall region and the cell adhesion-promoting fibrous microwell region. Because of these differences in the chemical natures and topological structures between the two domains, the hydrogel-incorporated fibrous scaffolds developed in this study possess the capability for spatial control of hMSCs within the selected areas. Figure 4c further demonstrates the presence of hMSCs on fiber region of hydrogel micropattern-incorporated fibrous scaffold

Loading and Release of Growth Factors. In addition to excellent non-fouling properties, PEG hydrogels have been shown to be an excellent matrix for encapsulation of various proteins due to their high water contents.[52,53] Therefore, PEG hydrogel micropatterns could be used not only for spatial control of cell growth but also to carry out other active functions such as sustained delivery of various proteins. On the other hands, electrospun fibers have shown good potential for

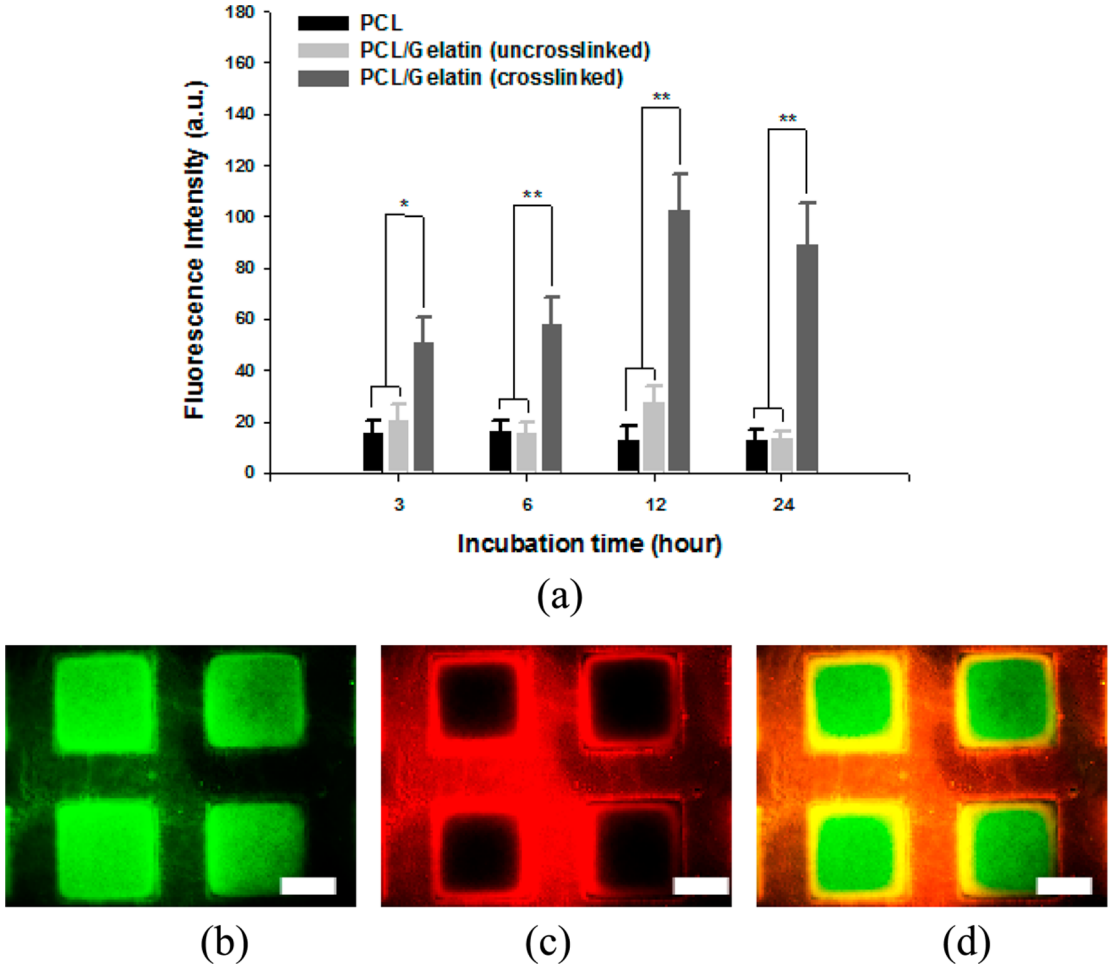

Figure 5. Loading of bFGF and BMP-2 into scaffolds. (a) Change of fluorescence intensity with incubation time by adsorption of Alexa 488-bFGF onto PCL/gelatin fibers. (b) Fluorescence image (green channel) of scaffold incubated with Alexa 488-bFGF for 12 h. (c) Fluorescence image (red channel) showing hydrogel micropatterns entrapping Alexa 594-BMP-2. (d) Fluorescence image of dual growth factor-loaded scaffold. Alexa 488-bFGF was immobilized onto PCL/gelatin fibers (green region), while Alexa 594-BMP-2 was entrapped within hydrogel micropattern (red region). Scale bar is 300 μm.

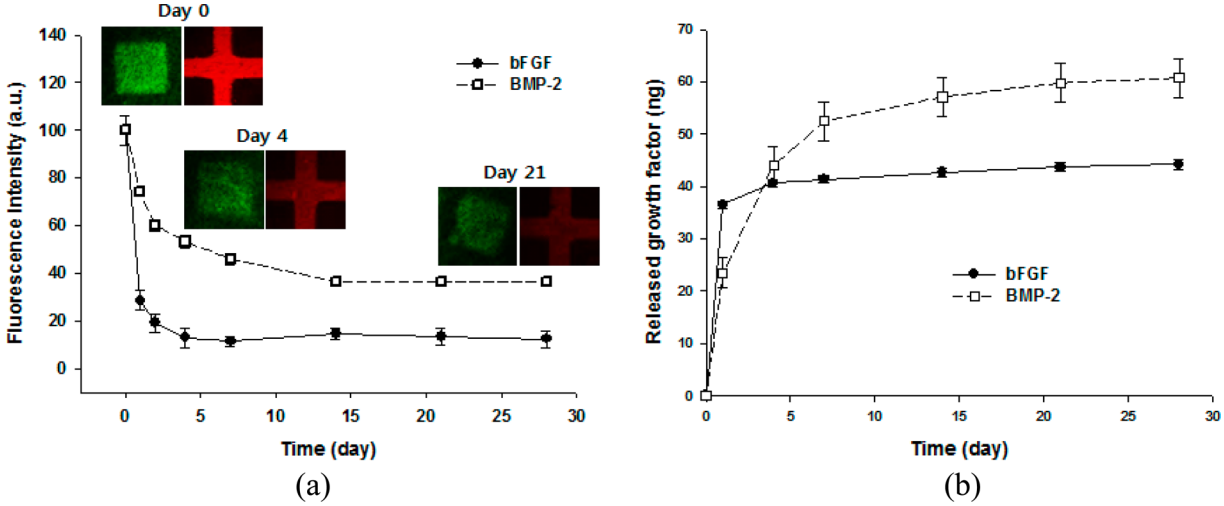

Figure 6. Release behaviors of bFGF and BMP-2 from scaffolds. (a) Change of fluorescence intensity in hydrogel and fiber region by release of bFGF and BMP-2 (green, bFGF; red, BMP-2). (b) Actual amount of released bFGF and BMP-2 from scaffolds.

drug delivery due to their large surface area and high porosity with an interconnected pore structures.[54] Considering the attractive features of hydrogels and electrospun fibers for protein delivery, it was expected that dual growth factor-releasing scaffolds could be generated by immobilizing one growth factor within the hydrogel matrix and another on the

fibers, where release of two growth factors are controlled independently by adjusting the properties of the hydrogels and the fibers. After crosslinked PCL/gelatin fibers were prepared, a BMP-2-containing hydrogel precursor solution was photopatterned to produce BMP-2-entrapped hydrogel micropatterns incorporated with PCL/gelatin fibers. Immersing the resultant scaffolds in bFGF solution after washing away non-entrapped BMP-2 led to immobilization of bFGF on the PCL/gelatin fiber regions via electrostatic interaction. Because the isoelectric points (pI) of gelatin (type B) and bFGF are 4.7−5.2 and 9.6, respectively, gelatin forms a polyion complex with bFGF within a range of pH 5−9.[55] Since gelatin is water-soluble, gelatin in un-cross-linked PCL/gelatin fiber was dissolved out by incubation with bFGF solution and resultant fibers would not have enough gelatins to interact with bFGF. Therefore, so little bFGF adsorbed to un-cross-linked fibers compared and crosslinked PCL/gelatin fibers could immobilize much more bFGF than other fibers via electrostatic interaction, as shown in Figure 5a.

The amount of immobilized bFGF on crosslinked PCL/gelatin fibers increased with incubation time and became saturated after 12 h (Figure 5a). Figure 5a also indicates that un-cross-linked PCL/gelatin fibers had similar bFGF-loading capacity to bare PCL fibers due to the dissolution of gelatin in the bFGF solution. The PEG hydrogel micropatterns effectively prevented non-specific adsorption of bFGF and negligible amounts of bFGF diffused into the hydrogel micropatterns during the incubation time (12 h), enabling selective immobilization of bFGF only at the fiber regions (Figure 5b). Figure 5c shows that BMP-2 was successfully entrapped within hydrogel micropatterns. Finally, we were able to fabricate scaffolds that consisted of BMP-entrapped hydrogel micropatterns (red fluorescence) and bFGF-immobilized fibers (green fluorescence), as shown in Figure 5d.

The release behaviors of bFGF and BMP-2 from the resultant scaffolds were first monitored by observing the change of fluorescence intensity in the hydrogel and fiber regions. Figure 6a indicates that the fluorescence intensity from both regions became weaker with incubation times because fewer amounts of growth factors remained in the scaffold, due to the release of the factors. Prior to this experiment, we confirmed that fluorescence intensity did not change if there was no growth factor and there was no photobleaching of fluorescence-labeled bFGF and BMP-2 over 4 weeks. Therefore, it could be concluded that decrease of fluorescence intensity from scaffolds solely resulted from the release of growth factors. In the case of bFGF on the fibers, there was a fast decrease of fluorescence intensity within 1 day and no more decrease occurred after 4 days. In contrast to bFGF, the rate of decrease of the fluorescence intensity was lower, and the decrease of the fluorescence intensity continued for 14 days, for BMP-2 in hydrogel. The release behaviors of bFGF and BMP-2 were further investigated quantitatively by measuring the cumulative amounts of growth factors over time. As shown in Figure 6b, similar behaviors were observed as with fluorescence intensity study. The release behavior of bFGF from the PCL/gelatin fibers showed a high initial burst of release within 1 day (82.6 %) followed by slow release until 4 days had passed. No significant release of bFGF was observed after 4 days of incubation. In contrast, BMP-2 release from the hydrogel micropatterns exhibited a lower initial burst (42.3 %) and a more sustained release pattern after that (86.4 % at day 7). Sustained release of BMP-2 continued even from day 7 to day 21, during which approximately 0.5 ng/day of BMP-2 was released from hydrogel micropatterns. Since approximately 60.65 ± 1.78 ng of bFGF and 108.01 ± 5.21 ng of BMP-2 were loaded into each scaffold, about 70% and 55% of bFGF and BMP-2 were released from the fiber and hydrogel, respectively after 28 days. Recent studies suggest that the ideal BMP-2 release strategy includes both an initial burst and a subsequent sustained release because the former helps to recruit osteoprogenitor cells to the delivery system and the latter promotes osteogenic differentiation.[56,57] Therefore, our system that showed an initial burst followed by sustained release of BMP-2 has the potential to synergistically enhance bone generation. The total amounts of bFGF and BMP-2 released from the scaffolds over a period of 4 weeks were 44.2 ± 0.9 ng and 60.7 ± 3.7 ng, respectively. These results indicate that our scaffolds have the capability to not only spatially localize the cells but also to control the release of multiple growth factors at different time periods. These advantages demonstrate that our scaffold has the potential for spatiotemporal control of stem cells. Similar behaviors were observed for the release of BMP-2 and bFGF from a scaffold containing only BMP-2 in the hydrogel micropatterns and a scaffold containing only bFGF on the fibers (data not shown), compared with release of each growth factor from scaffolds containing both BMP-2 and bFGF (shown in Figure 6b). This result demonstrates that presence of one growth factor had no effect on the release of the other growth factor. One important advantage of our hydrogel-incorporated fibrous scaffold is that various release profiles can be obtained independently for each growth factor by changing the properties of the hydrogel and the fibers separately. For example, the release of growth factor from PEG hydrogels can be controlled by changing the crosslinking density of hydrogels[58] and the release from fibers can be controlled by using different chemistries and processes for the preparation of the electrospun fibers. In this study, we used the above-obtained BMP-2 and bFGF-loaded scaffolds for the osteogenesis of hMSCs because it is known that a dose of bFGF during the early stages of osteogenesis and a sustained release of BMP-2 over long periods enhances the osteogenic induction of hMSC.

In Vitro Osteogenic Differentiation of hMSC. We investigated the effect of different combinations of growth factors on the proliferation and differentiation of hMSCs. We examined four scaffold groups: control, scaffold without growth factors; bFGF, scaffold containing only bFGF on the fibers; BMP-2, scaffold containing only BMP-2 in the hydrogel micropatterns; and bFGF/BMP-2, scaffold containing bFGF on the fibers and BMP-2 in the hydrogel. First, proliferation of hMSCs grown on different scaffold groups was investigated using MTT assays (Figure 7). During the first 7 days, the number of cells increased for all of the types of scaffolds, but there was no statistically significant difference between the different scaffolds. However, a significant difference in the number of viable cells was observed between the scaffolds with BMP-2 and without BMP-2 at 14 days and later. The control and bFGF groups had similar proliferation rates, showing a significant increase in the number of viable cells from 7 to 21 days, while the BMP-2 and bFGF/BMP-2 groups maintained similar numbers of cells from 7 to 14 days and a slight increase from 14 to 21 days. These results indicate that the early release of bFGF had no direct effect on cell proliferation, while the sustained release of BMP-2 suppressed the proliferation of hMSCs. The suppression of hMSC proliferation by BMP-2

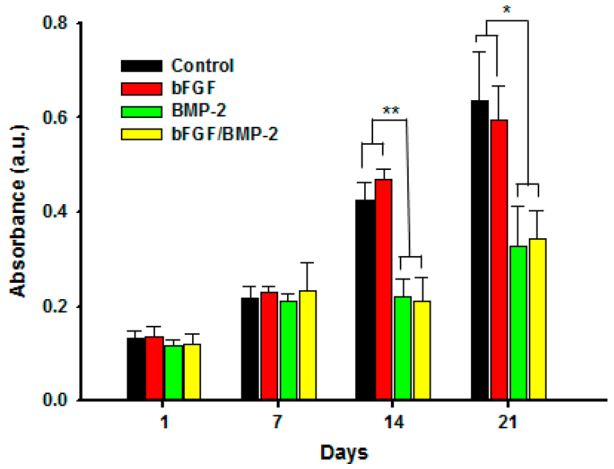

Figure 7. Effect of growth factors on the proliferation of hMSCs cultured on hydrogel micropattern-incorporated fibrous scaffolds.

does not inhibit osteogenesis of hMSCs because, as is widely known, cell proliferation decreases once cell differentiation develops.[59] Therefore, the suppression of hMSC proliferation on the BMP-2-containing scaffold could be interpreted to mean that BMP-2 induced the osteogenesis of the hMSC.

To investigate the osteogenic differentiation of hMSCs on different scaffolds, we stained the cells with alkaline phosphatase (ALP) after 14 days; ALP is known as an early marker for osteoblastic differentiation. Because the cells were spatially confined only within the fibrous region, ALP staining was observed in the fibrous region.

Faint ALP staining was detected on the scaffolds without BMP-2 (control and bFGF), but the staining was much more extensive in scaffolds containing BMP-2 (BMP-2 and bFGF/BMP-2) (Figure 8a). It was also observed that the bFGF/BMP-2 group showed higher levels of ALP staining than BMP-2 group. For the quantitative analysis of ALP levels, the relative activity of ALP was assessed for 21 days using pNPP as a substrate (Figure 8b). The ALP activity considerably increased at 14 days of culture only in the BMP-2-containing scaffolds (BMP-2 and bFGF/BMP-2). Considering that proliferation of hMSCs cultured in the BMP-2-containing scaffolds was suppressed at 14 days, this result is coincident with the proliferation study, suggesting that BMP-2 induced the early differentiation of hMSCs by suppressing cell proliferation. Although sequential delivery of bFGF and BMP-2 induced slightly better ALP activity than BMP-2-delivery alone at day

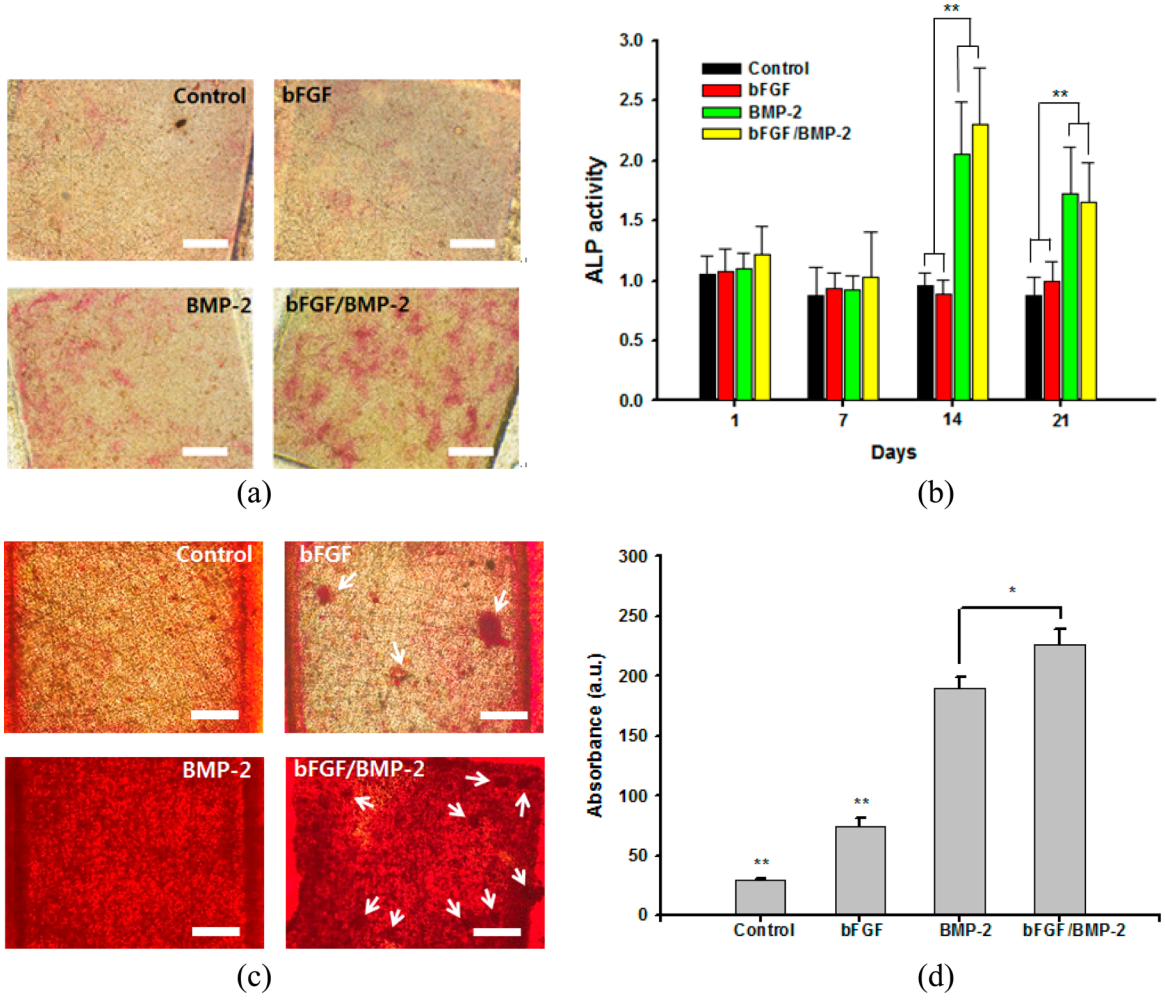

Figure 8. Osteogenic differentiation of hMSCs cultured on scaffold with different growth factor combinations. (a) ALP staining from cultured hMSCs after 14 days and (b) ALP activity as a function of culture periods. (c) ARS staining after 21 days (arrows indicate cell aggregates). Scale bar is 200 μm. (d) Quantitative analysis of the mineral deposition on day 21 by ARS staining.

dx.doi.org/10.1021/am501714k | ACS Appl. Mater. Interfaces 2014, 6, 9338−9348

14, it was not significantly different. There was also no significant difference between the control and the bFGF groups, indicating that bFGF alone did not contribute to the early osteogenesis of hMSCs. The osteogenic differentiation of hMSCs was further evaluated using Alizarin Red S (ARS); ARS is commonly used to quantify the mineralization of hMSCs because it binds to calcium salts selectively. As shown in Figure 8c, the scaffold that contained BMP-2 was more strongly stained than the control or the bFGF-only-containing scaffolds. Quantitative analysis of ARS staining also supported those results as shown Figure 8d, which indicated the significantly higher calcium deposition in bFGF/BMP-2 groups than other groups including BMP-2 only groups. Because the formation of calcium phosphate is the last stage marker for osteogenesis, These results confirmed that hMSCs cultured on the scaffolds capable of sequential delivery of bFGF and BMP-2 showed stronger osteogenic commitment (especially in mineralization) than those on scaffolds without any growth factors or scaffolds with single administration of either bFGF or BMP-2 under the same conditions. It should also be noted that cell aggregates were observed only on scaffolds containing bFGF (bFGF and bFGF/BMP-2 groups), as indicated by arrows in Figure 8c. The number of aggregates were 2 ± 1.1 and 9 ± 3.2 per one microwell for bFGF and bFGF/BMP-2 groups, respectively. Formation of cell aggregates is a positive result for the osteogenesis of hMSCs because it promotes mineralization without reducing the differentiation capability.[60] Although the hMSCs cultured on the BMP-2 groups showed evenly-distributed ARS stained region (Figure 8c), there was no definite cell aggregates. On the other hand, treatment with bFGF combined with BMP-2 increased the number of cell aggregates. It was known that FGF treatment promotes cell–cell adhesion during the early stages, which eventually increases cell aggregation.[61] Thus, the formation of cell aggregates in this study can be attributed to the initial release of bFGF from the scaffold.

■ CONCLUSION

We fabricated PCL/gelatin fibrous scaffolds incorporating PEG hydrogel micropatterns for potential applications to spatio-temporal control of hMSC differentiations. The resulting scaffolds were capable of controlling the spatial placement of hMSCs because hMSCs adhered only within the PCL/gelatin fiber region due to the non-adhesiveness of the PEG hydrogel. Furthermore, different growth factors could be separately loaded into the hydrogel micropatterns and the fibers in a single scaffold platform. Sequential delivery of bFGF and BMP-2 for osteogenesis of hMSC was achieved by a quick release of bFGF from the fibers and a slow and sustained release of BMP-2 from PEG hydrogel. The sequential delivery of bFGF and BMP-2 showed stronger osteogenic commitment in in vitro culture than those on scaffolds without any growth factors or scaffolds with single administration of either bFGF or BMP-2 under the same conditions.

■ AUTHOR INFORMATION

Corresponding Author

*Phone: 82-2-2123-5755. Fax: 82-2-312-6401. Email: wongun@yonsei.ac.kr.

Author Contributions

The manuscript was written through contributions of all authors. All authors have given approval to the final version of the manuscript.

Notes

The authors declare no competing financial interest.

■ ACKNOWLEDGMENTS

This work was supported by the National Research Foundation (NRF) grant funded by the Ministry of Science, ICT and Future Planning (MSIP) (2011-0022709, 2010K001430 "Converging Research Center Program", and R11-2007-050-03002-0 "Active Polymer Center for Pattern Integration at Yonsei University").

■ REFERENCES

(1) Fisher, O. Z.; Khademhosseini, A.; Langer, R.; Peppas, N. A. Bioinspired Materials for Controlling Stem Cell Fate. *Acc. Chem. Res.* **2009**, *43*, 419–428.

(2) Saha, K.; Pollock, J. F.; Schaffer, D. V.; Healy, K. E. Designing Synthetic Materials to Control Stem Cell Phenotype. *Curr. Opin. Chem. Biol.* **2007**, *11*, 381–387.

(3) Sands, R. W.; Mooney, D. J. Polymers to Direct Cell Fate by Controlling the Microenvironment. *Curr. Opin. Biotechnol.* **2007**, *18*, 448–453.

(4) Bettinger, C. J.; Langer, R.; Borenstein, J. T. Engineering Substrate Topography at the Micro- and Nanoscale to Control Cell Function. *Angew. Chem. Int. Ed.* **2009**, *48*, 5406–5415.

(5) Teo, B. K. K.; Ankam, S.; Chan, L. Y.; Yim, E. K. F. Nanotopography/Mechanical Induction of Stem-Cell Differentiation. *Methods Cell. Biol.* **2010**, *98*, 241–294.

(6) Barbucci, R.; Pasqui, D.; Wirsen, A.; Affrossman, S.; Curtis, A.; Tetta, C. Micro and Nano-structured Surfaces. *J. Mater. Sci.:Mater. Med.* **2003**, *14*, 721–725.

(7) Flemming, R. G.; Murphy, C. J.; Abrams, G. A.; Goodman, S. L.; Nealey, P. F. Effects of Synthetic Micro- and Nano-structured Surfaces on Cell Behavior. *Biomaterials* **1999**, *20*, 573–588.

(8) Kim, H. N.; Jiao, A.; Hwang, N. S.; Kim, M. S.; Kang, D.-H.; Kim, D.-H.; Suh, K.-Y. Nanotopography-Guided Tissue Engineering and Regenerative Medicine. *Adv. Drug Delivery. Rev.* **2013**, *65*, 536–558.

(9) Kriparamanan, R.; Aswath, P.; Zhou, A.; Tang, L. P.; Nguyen, K. T. Nanotopography: Cellular Responses to Nanostructured Materials. *J. Nanosci. Nanotechnol.* **2006**, *6*, 1905–1919.

(10) Lipski, A. M.; Jaquiery, C.; Choi, H.; Eberli, D.; Stevens, M.; Martin, I.; Chen, I. W.; Shastri, V. P. Nanoscale Engineering of Biomaterial Surfaces. *Adv. Mater.* **2007**, *19*, 553–557.

(11) Lord, M. S.; Modin, C.; Foss, M.; Duch, M.; Simmons, A.; Pedersen, F. S.; Milthorpe, B. K.; Besenbacher, F. Monitoring Cell Adhesion on Tantalum and Oxidised Polystyrene Using a Quartz Crystal Microbalance with Dissipation. *Biomaterials* **2006**, *27*, 4529–4537.

(12) Simon, K. A.; Burton, E. A.; Han, Y. B.; Li, J.; Huang, A.; Luk, Y. Y. Enhancing Cell Adhesion and Confinement by Gradient Nano-topography. *J. Am. Chem. Soc.* **2007**, *129*, 4892–4893.

(13) McMurray, R. J.; Gadegaard, N.; Tsimbouri, P. M.; Burgess, K. V.; McNamara, L. E.; Tare, R.; Murawski, K.; Kingham, E.; Oreffo, R. O. C.; Dalby, M. J. Nanoscale Surfaces for the Long-Term Maintenance of Mesenchymal Stem Cell Phenotype and Multi-potency. *Nat. Mater.* **2011**, *10*, 637–644.

(14) Beduer, A.; Vieu, C.; Arnauduc, F.; Sol, J. C.; Loubinoux, I.; Vaysse, L. Engineering of Adult Human Neural Stem Cells Differentiation Through Surface Micropatterning. *Biomaterials* **2012**, *33*, 504–514.

(15) Yang, K.; Jung, K.; Ko, E.; Kim, J.; Park, K. I.; Kim, J.; Cho, S. W. Nanotopographical Manipulation of Focal Adhesion Formation for Enhanced Differentiation of Human Neural Stem Cells. *ACS Appl. Mater. Interfaces* **2013**, *5*, 10529–10540.

(16) Agarwal, S.; Wendorff, J. H.; Greiner, A. Use of Electrospinning Technique for Biomedical Applications. *Polymer* **2008**, *49*, 5603−5621.
(17) Liao, S.; Ramakrishna, S.; Ramalingam, M. Development of Nanofiber Biomaterials and Stem Cells in Tissue Engineering. *J. Biomater. Tissue. Eng.* **2011**, *1*, 111−128.
(18) Kai, D.; Jin, G. R.; Prabhakaran, M. P.; Ramakrishna, S. Electrospun Synthetic and Natural Nanofibers for Regenerative Medicine and Stem Cells. *Biotechnol. J.* **2013**, *8*, 59−72.
(19) Folch, A.; Toner, M. Microengineering of Cellular Interactions. *Annu. Rev. Biomed. Eng.* **2000**, *2*, 227−256.
(20) Ito, Y. Surface Micropatterning to Regulate Cell Functions. *Biomaterials* **1999**, *20*, 2333−2342.
(21) Park, T. H.; Shuler, M. L. Intergration of Cell Culture and Microfabrication Technology. *Biotechnol. Prog.* **2003**, *19*, 243−253.
(22) Kane, R. S.; Takayama, S.; Ostuni, E.; Ingber, D. E.; Whitesides, G. M. Patterning Proteins and Cells Using Soft Lithography. *Biomaterials* **1999**, *20*, 2363−2376.
(23) Lee, H. J.; Nam, S. H.; Son, K. J.; Koh, W.-G. Micropatterned Fibrous Scaffolds Fabricated Using Electrospinning and Hydrogel Lithography: New Platforms to Create Cellular Micropatterns. *Sensors Actuators B* **2010**, *148*, 504−510.
(24) Jiang, L.; Zhang, M.; Li, J. X.; Wen, W. J.; Qin, J. H. Simple Localization of Nanofiber Scaffolds via SU-8 Photoresist and Their Use for Parallel 3D Cellular Assays. *Adv. Mater.* **2012**, *24*, 2191−2195.
(25) Lee, J.; Lee, S. Y.; Jang, J.; Jeong, Y. H.; Cho, D. W. Fabrication of Patterned Nanofibrous; Mats Using Direct-Write Electrospinning. *Langmuir* **2012**, *28*, 7267−7275.
(26) Lee, K.; Silva, E. A.; Mooney, D. J. Growth Factor Delivery-Based Tissue Engineering: General Approaches and a Review of Recent Developments. *J. R. Soc., Interface* **2011**, *8*, 153−170.
(27) Chung, H. J.; Park, T. G. Surface Engineered and Drug Releasing Pre-Fabricated Scaffolds for Tissue Engineering. *Adv. Drug Delivery. Rev.* **2007**, *59*, 249−262.
(28) Wang, D. A.; Varghese, S.; Sharma, B.; Strehin, I.; Fermanian, S.; Gorham, J.; Fairbrother, D. H.; Cascio, B.; Elisseeff, J. H. Multifunctional Chondroitin Sulphate for Cartilage Tissue-Biomaterial Integration. *Nat. Mater.* **2007**, *6*, 385−392.
(29) Salgado, A. J.; Coutinho, O. P.; Reis, R. L. Bone Tissue Engineering: State of the Art and Future Trends. *Macromol. Biosci.* **2004**, *4*, 743−765.
(30) de Groot, K. Carriers that Concentrate Native Bone Morphogenetic Protein In Vivo. *Tissue Eng.* **1998**, *4*, 337−341.
(31) Chen, F. M.; Zhang, M.; Wu, Z. F. Toward Delivery of Multiple Growth Factors in Tissue Engineering. *Biomaterials* **2010**, *31*, 6279−6308.
(32) Richardson, T. P.; Peters, M. C.; Ennett, A. B.; Mooney, D. J. Polymeric System for Dual Growth Factor Delivery. *Nat. Biotechnol.* **2001**, *19*, 1029−1034.
(33) Holland, T. A.; Bodde, E. W. H.; Cuijpers, V. M. J. I.; Baggett, L. S.; Tabata, Y.; Mikos, A. G.; Jansen, J. A. Degradable Hydrogel Scaffolds for In Vivo Delivery of Single and Dual Growth Factors in Cartilage Repair. *Osteoarthr. Cartilage* **2007**, *15*, 187−197.
(34) Hao, X. J.; Silva, E. A.; Mansson-Broberg, A.; Grinnemo, K. H.; Siddiqui, A. J.; Dellgren, G.; Wardell, E.; Brodin, L. A.; Mooney, D. J.; Sylven, C. Angiogenic Effects of Sequential Release of VEGF-A(165) and PDGF-BB with Alginate Hydrogels after Myocardial Infarction. *Cardiovasc. Res.* **2007**, *75*, 178−185.
(35) Schmidmaier, G.; Wildemann, B.; Gabelein, T.; Heeger, J.; Kandziora, F.; Haas, N. P.; Raschke, M. Synergistic Effect of IGF-I and TGF-β 1 on Fracture Healing in Rats. Single versus Combined Application of IGF-I and TGF-beta 1. *Acta Orthop. Scand.* **2003**, *74*, 604−610.
(36) Simmons, C. A.; Alsberg, E.; Hsiong, S.; Kim, W. J.; Mooney, D. J. Dual Growth Factor Delivery and Controlled Scaffold Degradation Enhance In Vivo Bone Formation by Transplanted Bone Marrow Stromal Cells. *Bone* **2004**, *35*, 562−569.
(37) Basmanav, F. B.; Kose, G. T.; Hasirci, V. Sequential Growth Factor Delivery from Complexed Microspheres for Bone Tissue Engineering. *Biomaterials* **2008**, *29*, 4195−4204.
(38) Nakamura, Y.; Tensho, K.; Nakaya, H.; Nawata, M.; Okabe, T.; Wakitani, S. Low Dose Fibroblast Growth Factor-2 (FGF-2) Enhances Bone Morphogenetic Protein-2 (BMP-2)-Induced Ectopic Bone Formation in Mice. *Bone* **2005**, *36*, 399−407.
(39) Huang, Z.; Ren, P.-G.; Ma, T.; Smith, R. L.; Goodman, S. B. Modulating Osteogenesis of Mesenchymal Stem Cells by Modifying Growth Factor Availability. *Cytokine* **2010**, *51*, 305−310.
(40) Wang, L.; Huang, Y.; Pan, K.; Jiang, X.; Liu, C. Osteogenic Responses to Different Concentrations/Ratios of BMP-2 and bFGF in Bone Formation. *Ann. Biomed. Eng.* **2010**, *38*, 77−87.
(41) Huang, Z.; Nelson, E. R.; Smith, R. L.; Goodman, S. B. The Sequential Expression Profiles of Growth Factors from Osteroprogenitors to Osteoblasts In Vitro. *Tissue Eng.* **2007**, *13*, 2311−2320.
(42) Hanada, K.; Dennis, J. E.; Caplan, A. I. Stimulatory Effects of Basic Fibroblast Growth Factor and Bone Morphogenetic Protein-2 on Osteogenic Differentiation of Rat Bone Marrow-Derived Mesenchymal Stem Cells. *J. Bone Miner. Res.* **1997**, *12*, 1606−1614.
(43) Maegawa, N.; Kawamura, K.; Hirose, M.; Yajima, H.; Takakura, Y.; Ohgushi, H. Enhancement of Osteoblastic Differentiation of Mesenchymal Stromal Cells Cultured by Selective Combination of Bone Morphogenetic Protein-2 (BMP-2) and Fibroblast Growth Factor-2 (FGF-2). *J. Tissue Eng. Regener. Med.* **2007**, *1*, 306−313.
(44) Vonau, R. L.; Bostrom, M. P. G.; Aspenberg, P.; Sams, A. E. Combination of Growth Factors Inhibits Bone Ingrowth in the Bone Harvest Chamber. *Clin. Orthop. Relat. Res.* **2001**, 243−251.
(45) Lee, H. J.; Kim, H.-S.; Kim, H. O.; Koh, W.-G. Micropatterns of Double-Layered Nanofiber Scaffolds with Dual Functions of Cell Patterning and Metabolite Detection. *Lab Chip* **2011**, *11*, 2849−2857.
(46) Lee, Y.; Lee, H. J.; Son, K. J.; Koh, W.-G. Fabrication of Hydrogel-Micropatterned Nanofibers for Highly Sensitive Microarray-Based Immunosensors Having Additional Enzyme-Based Sensing Capability. *J. Mater. Chem.* **2011**, *21*, 4476−4483.
(47) Zhang, Y. Z.; Venugopal, J.; Huang, Z. M.; Lim, C. T.; Ramakrishna, S. Crosslinking of the Electrospun Gelatin Nanofibers. *Polymer* **2006**, *47*, 2911−2917.
(48) Quinn, C. P.; Pathak, C. P.; Heller, A.; Hubbell, J. A. Photo-Crosslinked Copolymers of 2-Hydroxyethyl Methacrylate, Poly-(ethylene glycol) tetra-acrylate and Ethylene Dimethacrylate for Improving Biocompatibility of Biosensors. *Biomaterials* **1995**, *16*, 389−396.
(49) Park, S.; Ahn, S. H.; Lee, H. J.; Chung, U. S.; Kim, J. H.; Koh, W. G. Mesoporous TiO_2 as a Nanostructured Substrate for Cell Culture and Cell Patterning. *RSC Adv.* **2013**, *3*, 23673−23680.
(50) Kim, M. S.; Shin, Y. M.; Lee, J.-h.; Kim, S. I.; Nam, Y. S.; Shin, C. S.; Shin, H. Release Kinetics and In Vitro Bioactivity of Basic Fibroblast Growth Factor: Effect of the Thickness of Fibrous Matrices. *Macromol. Biosci.* **2011**, *11*, 122−130.
(51) Ma, Z.; He, W.; Yong, T.; Ramakrishna, S. Grafting of Gelatin on Electrospun Poly(caprolactone) Nanofibers to Improve Endothelial Cell Spreading and Proliferation and to Control Cell Orientation. *Tissue Eng.* **2005**, *11*, 1149−1158.
(52) Mellott, M. B.; Searcy, K.; Pishko, M. V. Release of Protein from Highly Cross-linked Hydrogels of Poly(ethylene glycol) diacrylate Fabricated by UV Polymerization. *Biomaterials* **2001**, *22*, 929−941.
(53) Jang, E.; Koh, W. G. Multiplexed Enzyme-Based Bioassay within Microfluidic Devices Using Shape-Coded Hydrogel Microparticles. *Sensor Actuators B* **2010**, *143*, 681−688.
(54) Xie, J. W.; Li, X. R.; Xia, Y. N. Putting Electrospun Nanofibers to Work for Biomedical Research. *Macromol. Rapid Commun.* **2008**, *29*, 1775−1792.
(55) Muniruzzaman, M.; Tabata, Y.; Ikada, Y. Complexation of Basic Fibroblast Growth Factor with Gelatin. *J. Biomater. Sci., Polym. Ed.* **1998**, *9*, 459−473.
(56) Brown, K. V.; Li, B.; Guda, T.; Perrien, D. S.; Guelcher, S. A.; Wenke, J. C. Improving Bone Formation in a Rat Femur Segmental

Defect by Controlling Bone Morphogenetic Protein-2 Release. *Tissue Eng. A* **2011**, *17*, 1735−1746.
(57) Fiedler, J.; Roderer, G.; Gunther, K. P.; Brenner, R. E. BMP-2, BMP-4, and PDGF-bb Stimulate Chemotactic Migration of Primary Human Mesenchymal Progenitor Cells. *J. Cell. Biochem.* **2002**, *87*, 305−312.
(58) Weber, L. M.; Lopez, C. G.; Anseth, K. S. Effects of PEG Hydrogel Crosslinking Density on Protein Diffusion and Encapsulated Islet Survival and Function. *J. Biomed. Mater. Res., Part A* **2009**, *90A*, 720−729.
(59) Stein, G. S.; Lian, J. B.; Owen, T. A. Relationship of Cell Growth to the Regulation of Tissue-Specific Gene Expression during Osteoblast Differentiation. *FASEB J.* **1990**, *4*, 3111−23.
(60) Facer, S. R.; Zaharias, R. S.; Andracki, M. E.; Lafoon, J.; Hunter, S. K.; Schneider, G. B. Rotary Culture Enhances Pre-osteoblast Aggregation and Mineralization. *J. Dent. Res.* **2005**, *84*, 542−547.
(61) Debiais, F.; Lemonnier, J.; Hay, E.; Delannoy, P.; Caverzasio, J.; Marie, P. J. Fibroblast Growth Factor-2 (FGF-2) Increases N-cadherin Expression Through Protein Kinase C and Src-Kinase Pathways in Human Calvaria Osteoblasts. *J. Cell. Biochem.* **2001**, *81*, 68−81.